

# Nature does not rely on long-lived electronic quantum coherence for photosynthetic energy transfer

Hong-Guang Duan<sup>a,b,c</sup>, Valentyn I. Prokhorenko<sup>a</sup>, Richard J. Cogdell<sup>d</sup>, Khuram Ashraf<sup>d</sup>, Amy L. Stevens<sup>a,c,e,f</sup>, Michael Thorwart<sup>b,c,1</sup>, and R. J. Dwayne Miller<sup>a,c,e,f,1</sup>

<sup>a</sup>Atomically Resolved Dynamics Department, Max Planck Institute for the Structure and Dynamics of Matter, 22761 Hamburg, Germany; <sup>b</sup>I. Institut für Theoretische Physik, Universität Hamburg, 20355 Hamburg, Germany; <sup>c</sup>The Hamburg Center for Ultrafast Imaging, 22761 Hamburg, Germany; <sup>d</sup>Institute of Molecular, Cell, and Systems Biology, College of Medical, Veterinary, and Life Science, University of Glasgow, Glasgow G12 8QQ, United Kingdom; <sup>e</sup>Department of Chemistry, University of Toronto, Toronto, ON, Canada M5S 3H6; and <sup>f</sup>Department of Physics, University of Toronto, Toronto, ON, Canada M5S 3H6

Edited by Shaul Mukamel, University of California, Irvine, CA, and approved June 1, 2017 (received for review February 9, 2017)

During the first steps of photosynthesis, the energy of impinging solar photons is transformed into electronic excitation energy of the light-harvesting biomolecular complexes. The subsequent energy transfer to the reaction center is commonly rationalized in terms of excitons moving on a grid of biomolecular chromophores on typical timescales <100 fs. Today's understanding of the energy transfer includes the fact that the excitons are delocalized over a few neighboring sites, but the role of quantum coherence is considered as irrelevant for the transfer dynamics because it typically decays within a few tens of femtoseconds. This orthodox picture of incoherent energy transfer between clusters of a few pigments sharing delocalized excitons has been challenged by ultrafast optical spectroscopy experiments with the Fenna–Matthews–Olson protein, in which interference oscillatory signals up to 1.5 ps were reported and interpreted as direct evidence of exceptionally long-lived electronic quantum coherence. Here, we show that the optical 2D photon echo spectra of this complex at ambient temperature in aqueous solution do not provide evidence of any long-lived electronic quantum coherence, but confirm the orthodox view of rapidly decaying electronic quantum coherence on a timescale of 60 fs. Our results can be considered as generic and give no hint that electronic quantum coherence plays any biofunctional role in real photoactive biomolecular complexes. Because in this structurally well-defined protein the distances between bacteriochlorophylls are comparable to those of other light-harvesting complexes, we anticipate that this finding is general and directly applies to even larger photoactive biomolecular complexes.

2D spectroscopy | exciton | photosynthesis | Fenna–Matthews–Olson protein | quantum coherence

The principle laws of physics undoubtedly also govern the principle mechanisms of biology. The animate world consists of macroscopic and dynamically slow structures with a huge number of degrees of freedom, such that the laws of statistical mechanics apply. Conversely, the fundamental theory of the microscopic building blocks is quantum mechanics. The physics and chemistry of large molecular complexes may be considered as a bridge between the molecular world and the formation of living matter. A fascinating question since the early days of quantum theory is on the borderline between the atomistic quantum world and the classical world of biology. Clearly, the conditions under which matter displays quantum features or biological functionality are contrarious. Quantum coherent features only become apparent when systems with a few degrees of freedom with a preserved quantum mechanical phase relation of a wave function are well shielded from environmental fluctuations that otherwise lead to rapid dephasing. This dephasing mechanism is very efficient at ambient temperatures, at which biological systems operate. Also, the function of biological macromolecular systems relies on their embedding in a “wet” and highly polar solvent environment, which is again hostile to any quantum coherence.

Therefore, the common view of multichromophoric Förster resonance energy transfer has been developed in which excitons are quantum-mechanically delocalized over a few neighboring pigments (1, 2), but a quantum coherent phase relation between the clusters involved in any biologically relevant dynamical process is rapidly destroyed on a sub-100-fs timescale. The transport is dominated by dipolar coupling between the sites with different energies, such that it is spatially directed and naturally leads to energy relaxation and flow to the reaction center. The nature of any quantum coherence is short-lived and could, at most, only involve a few neighboring sites—a view that is distinctively different from that of a largely quantum coherent process as implied by very long-lived electronic coherence living as long as proposed (3–5).

In recent years, ultrafast nonlinear 2D optical spectroscopy (6–8) has made it possible to challenge the orthodox view of the energy transfer because it can provide direct access to the couplings between excitonic states. A prominent energy transfer complex, which is simple enough to provide clean experimental spectroscopic data, is the Fenna–Matthews–Olson (FMO) protein (9). In 2007, the oscillatory beatings observed in the

## Significance

We have revisited the 2D spectroscopy of the excitation energy transfer in the Fenna–Matthews–Olson (FMO) protein. Based on 2D spectroscopic signatures, the energy transfer dynamics in the FMO protein has been argued to be supported by long-lived electronic quantum coherence on timescales up to 1.5 ps. In contrast, our analysis, based on experimental data and confirmed by theoretical calculations, shows that the electronic decoherence occurs within 60 fs, in agreement with typical dephasing times in systems under these conditions. Given the relatively well-defined structure of the FMO protein, and comparative couplings between chlorophylls to other photosynthetic systems, the observed extremely fast decoherence should be viewed as general, bringing to question any significant quantum coherent transport contributions to photosynthesis.

Author contributions: V.I.P., M.T., and R.J.D.M. designed research; H.-G.D., V.I.P., A.L.S., and M.T. performed research; R.J.C. and K.A. contributed new reagents/analytic tools; H.-G.D., V.I.P., A.L.S., M.T., and R.J.D.M. analyzed data; and H.-G.D., V.I.P., R.J.C., M.T., and R.J.D.M. wrote the paper.

Conflict of interest statement: H.-G.D., V.I.P., and M.T. have a common publication in the *New Journal of Physics* with Shaul Mukamel as coauthor in 2015 on two-dimensional spectroscopy of a simple dye molecule. M.T. has a common publication with Shaul Mukamel in *The Journal of Chemical Physics* in 2014 on excitation energy transfer in molecules with orthogonal dipoles.

This article is a PNAS Direct Submission.

Freely available online through the PNAS open access option.

<sup>1</sup>To whom correspondence may be addressed. Email: michael.thorwart@physik.uni-hamburg.de or dwayne.miller@mpsd.mpg.de.

This article contains supporting information online at [www.pnas.org/lookup/suppl/doi:10.1073/pnas.1702261114/-DCSupplemental](http://www.pnas.org/lookup/suppl/doi:10.1073/pnas.1702261114/-DCSupplemental).



(indicated in Fig. 1A by the black line) with a fitted Lorentzian profile yielding a FWHM of  $\Delta_{\text{hom}} = 175 \text{ cm}^{-1}$ , which corresponds to an electronic dephasing time of  $\tau_{\text{hom}} = [\pi c \Delta_{\text{hom}}]^{-1} = 60 \text{ fs}$  ( $c$  is the speed of light). We note that the negative peaks in Fig. 1A and B are due to a mixed photon echo signal with contributions from the solvent and the excited state absorption (6–8). The mixed photon echo signal gives 50 counts (cts) for the solvated FMO, and, in the absence of FMO, we have detected 10 cts. The solvent signal completely disappears for waiting times up to 20–30 fs. Therefore, we estimate that the solvent (FMO excited state absorption) contribution to the negative peak is  $\sim 20\%$  (80%). Furthermore, the magnitude of the off-diagonal peaks in the upper left region of the 2D spectra remarkably increases for growing waiting times. The spectrum becomes strongly elongated along the  $\omega_{\tau}$  coordinate and reveals an efficient energy transfer between the FMO pigments (6–8). The progressions ranging from the central peak at  $\omega_{\tau} = \omega_t = 12,400 \text{ cm}^{-1}$  to the region  $\omega_{\tau} = 13,500 \text{ cm}^{-1}$ ,  $\omega_t = 12,400 \text{ cm}^{-1}$  indicate a vibrational relaxation of the localized vibrational modes of the bacteriochlorophylls. In addition, we clearly observe a fast decay of the central peak amplitude within the first 1–2 ps, induced by thermally fluctuating electric fields from the polar protein environment.

The energy transfer pathways and the associated timescales are revealed by a multidimensional global analysis (43) of consecutive 2D spectra at different waiting times  $T$ , arranged in a 3D array  $S(\omega_{\tau}, \omega_t, T)$  (for a detailed description, see supporting information in ref. 44). This results in 2D decay-associated spectra (2DDAS)  $A_i(\omega_{\tau}, \omega_t)$ , which are shown in Fig. 2A (Left, analyzed experimental spectra; Right, analyzed theoretical data; see also SI Appendix for more details). We have resolved four different energy transfer timescales. The shortest decay time,  $\tau_1 = 90 \text{ fs}$ , is mainly associated to the electronic dephasing of the diagonal peak at  $12,500 \text{ cm}^{-1}$ . Furthermore, a strong negative off-diagonal peak at ( $\omega_{\tau} = 12,500 \text{ cm}^{-1}$ ,  $\omega_t = 12,000 \text{ cm}^{-1}$ ) indicates a rapid loss of absorption in the 2D spectra. This feature illustrates contributions from the energy transfer process from the excitonic states located around  $12,500 \text{ cm}^{-1}$  to the lower

ones at  $12,000 \text{ cm}^{-1}$ . The second 2DDAS, associated with a lifetime of  $\tau_2 = 750 \text{ fs}$ , displays a similar feature, but with slightly broader peaks and a noticeable extension to the blue spectral side. The third ( $\tau_3 = 7.0 \text{ ps}$ ) and fourth ( $\tau_4 = \infty$ ) components of the 2DDAS only show one diagonal peak at the central position of  $12,200 \text{ cm}^{-1}$  with rather broad peaks. This observation indicates a thermal relaxation of the pigments inside the FMO protein. Our findings qualitatively agree with those in ref. 17, with all our dephasing times being shorter, which is due the difference in temperature between 77 K and the present studies under ambient conditions.

Next, we address the question of long-lived coherent oscillations in off-diagonal signals in the 2D spectra. We have analyzed the residuals obtained after removing the underlying slow kinetics from the 3D dataset  $S(\omega_{\tau}, \omega_t, T)$ . Their Fourier transform provides a 3D spectrum of the possible vibrations. The most intense of them, with the amplitudes above the noise threshold, are plotted in SI Appendix, Figs. S9 and S10. As a result of our model, all of the exciton states in the FMO complex are located in the frequency region of  $12,123$ – $12,615 \text{ cm}^{-1}$ . Hence, the largest oscillation frequency that can be expected from the beatings between them is  $\sim 490 \text{ cm}^{-1}$ . However, the lowest oscillation frequency that we found in the residuals lies well above ( $\sim 600 \text{ cm}^{-1}$ ). Hence, we can safely conclude that the origin of these oscillations is not due to interference between the excitonic states.

A cross-correlation analysis (44) of the residuals across the diagonal  $\omega_{\tau} = \omega_t$  in a delay time window up to 2 ps yields a 2D correlation spectrum shown in Fig. 2B, where the (negative) positive values indicate (anti)correlated residuals. We find two strong negative peaks, which proves on the basis of refs. 45 and 46 that the oscillations in this region are related to vibrational coherence. Moreover, we clearly observe two negative peaks at the frequencies  $12,400 \text{ cm}^{-1}$  and  $13,300 \text{ cm}^{-1}$ . They can be associated to strong localized vibrational modes of the bacteriochlorophylls, which follows from the vibrational progression in the absorption spectrum (SI Appendix, Fig. S24).

To underpin the vibrational origin of the oscillations with rather small amplitudes, we consider the time evolution of the

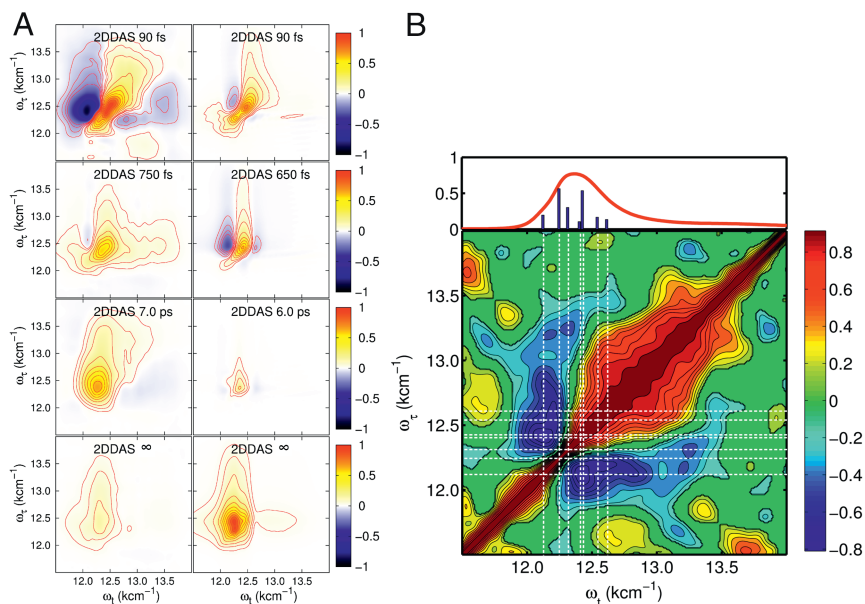


**Fig. 2.** (A) The 2DDAS. A, Left shows the experimental results, and A, Right shows the theoretically calculated spectra. The four resulting associated decay times  $\tau_{1,\dots,4}$  are indicated in the spectra. (B) The 2D correlation map of residuals obtained from the series of experimental spectra after subtracting the kinetics by the global fitting procedure. The red line on top is the measured absorption spectrum of the FMO trimer, and the blue bars mark the stick spectrum of the FMO model. The white dashed lines mark the exciton energies, which are used to overlap with the correlation map.

two off-diagonal signals located at the pair of frequencies  $12,300\text{ cm}^{-1}$  and  $12,600\text{ cm}^{-1}$ , marked by the red and blue squares in Fig. 1A. We consider the results of the theoretical modeling, which explicitly only includes an overdamped vibrational mode (with a vibrational lifetime of  $\tau_V = 15\text{ fs}$ ; *SI Appendix*), but does not include underdamped vibrational states of the bacteriochlorophylls. Hence, any calculated oscillations occurring out to long time must originate from possible beatings of the electronic dynamics due to a coherent coupling between the excitonic states. This feature helps to uniquely determine the origin of the oscillations observed in the experimental spectra. The results shown in Fig. 3A and B illustrate that any electronic coherence between excitonic states vanishes within a dephasing time window of  $\sim 60\text{ fs}$ . It is interesting to point out that this value of the dephasing time agrees with the time of the dephasing measured by the antidiagonal bandwidth of the 2D spectrum at  $T = 0\text{ fs}$ . In fact, when the fluctuations are fast, the timescales of homogeneous and inhomogeneous broadening are well separated, and we are in the fast modulation or homogeneous limit. The resulting exciton dynamics is then Markovian, and, in this limit, the antidiagonal (or homogeneous) line width and the electronic dephasing time coincide (47, 48). The Markovian character of the exciton dynamics is revealed by the exponentially decaying frequency correlation function (48), which can be extracted by measuring the ellipse eccentricity (49) of the 2D spectra as a function of the waiting time (*SI Appendix*, Fig. S13). In addition, in the numerically exact calculation of ref. 50, the non-Markovianity measure of the FMO exciton dynamics has been calculated to be zero. Furthermore, the excellent agreement between the experimental and theoretical values of the antidiagonal bandwidth demonstrates the validity of our model to capture the damping induced by the thermal noise. In addition, our direct observation of the homogeneous linewidth in this fast modulation limit is in agreement with the independent FMO data of ref. 17 (*SI Appendix*, Fig. S6). This study finds an  $\sim 100\text{ cm}^{-1}$  homogeneous line width estimated from the low-temperature data at  $77\text{ K}$ . The resulting electronic dephasing time can be calculated from our model with all of the parameters kept unchanged except the temperature. We find  $110\text{ fs}$  (*SI Appendix*, Fig. S7). In fact, if long-lived electronic coherence were operating on the  $1\text{-ps}$  timescale as claimed perviously (3), the electronic dephasing should be significantly reduced due to a weaker exciton-phonon interaction. The corresponding antidiagonal line width of the 2D spectrum would have to be on the order of  $10\text{ cm}^{-1}$  (*SI Appendix*, Fig. S8) and would appear as an extremely (unrealistically) sharp ridge in the inhomogeneously broadened 2D spectrum. The lack of this feature conspicuously points to the misassignment

of the long-lived features to long-lived electronic coherences, which, as now established in the present work, is due to weak vibrational coherences. The frequencies of these oscillations, their lifetimes, and amplitudes all match those expected for molecular modes (51, 52), and not long-lived electronic coherences.

For a comparison with the previous experimental work [at the temperature  $277\text{ K}$  ( $4^\circ\text{C}$ ) of ref. 4], we have extracted from our measured 2D spectra the time evolution of the “cross-peak” located at  $\omega_\tau = 12,350\text{ cm}^{-1}$ ,  $\omega_t = 12,200\text{ cm}^{-1}$  (spectral position marked by a black cross in Fig. 1A). As follows from Fig. 3C (see also *SI Appendix*), no long-lived beatings and associated electronic coherence can be observed at this position in the measured 2D spectra. Within the available experimental signal-to-noise ratio, we can conclude that there are no oscillations with amplitudes  $>5\%$  of the signal. They may be interpreted as weak vibrational coherence, consistent with earlier findings (41) for a much smaller excitonically coupled system (a dimer) with strong vibronic coupling.

## Conclusion

The present work provides a full analysis of possible electronic state couplings, decay-associated spectra, signs/amplitudes of off-diagonal features, and, most telling, the directly determined homogeneous lineshape, and thus shows that the previous assignment of weak long-lived oscillatory signals in 2D spectra to long-lived electronic coherences is incorrect. There is no long-range coherent energy transport occurring in the FMO complex and, in all cases, is not needed to explain the overall efficiency of energy transfer. This finding constitutes the main result of our work and confirms the orthodox picture of rapidly decaying electronic coherence on a timescale of  $60\text{ fs}$  in the exciton dynamics in the FMO protein complex at ambient temperature. In turn, contributions of quantum coherence to biological functionality under ambient conditions in natural light-harvesting units is extremely unlikely, a finding being in line with our previous study of the light-harvesting complex LHCII (44). Because the FMO complex is rather small and a structurally quite well-defined protein, with the distances between bacteriochlorophylls comparable to other natural light-harvesting systems, we anticipate that this finding is generic and also applies to even larger photoactive biomolecular complexes.

## Materials and Methods

**Experimental Setup.** Ultrashort coherent light pulses were generated by a home-built noncollinear optical parametric amplifier pumped by a commercial femtosecond laser Pharos (Light Conversion). A broadband spectrum with a FWHM of  $100\text{ nm}$  was centered at the wavelength of  $770\text{ nm}$

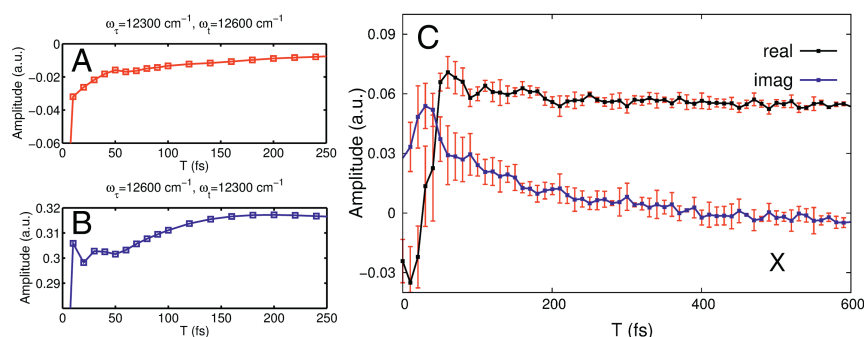


**Fig. 3.** (A and B) Time evolution of the real part of the calculated 2D photon echo signal at the spectral positions  $\omega_\tau = 12,300\text{ cm}^{-1}$ ,  $\omega_t = 12,600\text{ cm}^{-1}$  marked by a red square in Fig. 1A (A) and for  $\omega_\tau = 12,600\text{ cm}^{-1}$ ,  $\omega_t = 12,300\text{ cm}^{-1}$  marked by a blue square in Fig. 1A (B). It is apparent that a minimal amount of electronic coherence only survives up to  $\sim 60\text{ fs}$ . (C) The real (black) and imaginary (blue) part of the experimentally measured time trace at the same spectral position (black cross in Fig. 1A)  $\omega_\tau = 12,350\text{ cm}^{-1}$ ,  $\omega_t = 12,200\text{ cm}^{-1}$  as measured in ref. 4, however, measured here at  $296\text{ K}$ . The error bars indicate the SD obtained after averaging four datasets. The imaginary part is vertically shifted by  $0.035$  for clarity. a.u., arbitrary units.

and overlapped the  $Q_y$  absorption band of the FMO antenna complex (*SI Appendix, Fig. S2A*). The laser pulses were compressed to the transform-limited with the pulse duration of 16 fs FWHM by a combination of a prism compressor (F2) and a deformable mirror shaper (OKO Technologies). Their temporal profiles were characterized by means of the frequency-resolved optical gating (FROG) measured in situ by using a 1-mm fused silica window. The measured FROG traces were analyzed by using a commercial program, FROG3 (Femtosecond Technologies). The 2D spectra were collected in an all-reflective 2D spectrometer based on a diffractive optic (Holoeye) with a phase stability of  $\lambda/160$ , whose configuration is described elsewhere (53), equipped with the Scientech spectrometer model 9055 and a high-sensitive CCD linear array camera (Entwicklungsbüro Stresing). To avoid possible annihilation of excitons in the FMO trimer, the excitation energy was kept at  $<12$  nJ per beam. Under this excitation condition, the magnitude of the homodyne photon-echo signal was proportional to the third power of the incoming pulse energy, which confirms the regime of linear excitation (*SI Appendix, Fig. S2B*). The 2D spectra were collected at each fixed waiting time  $T$  by scanning the delay  $\tau = t_1 - t_2$  in the range of  $[-128$  fs,  $128$  fs] with a delay step of 1 fs. At each delay point, 150 spectra were averaged. The waiting time  $T = t_3 - t_2$  was linearly scanned within the range of  $0 - 2$  ps in steps of 10 fs and with logarithmically spaced delay time steps up to 10 ps.

**Sample Preparation and Measuring Condition.** The FMO protein was isolated from the green sulfur bacteria *C. tepidum* (see *SI Appendix* for details). Before each series of measurements, the sample was filtered with a  $0.2 \mu\text{m}$  filter to reduce light scattering. The absorption spectrum was recorded by using a Shimadzu spectrometer (UV-2600) in a cell of 1-mm optical path length. To avoid the influence of the sample degradation (see *SI Appendix* for details), the cell in the 2D setup was placed on a precise 2D translator and moved at a speed of  $\sim 20$  cm/s in both directions. The excitation spot diameter on the sample was  $\sim 80 \mu\text{m}$ . In the experiments, we used a 1-mm quartz cell (Starna). We did not detect any noticeable difference of the measured spectra when a  $0.5\text{-mm}$  cell was used.

**Theoretical Model.** We considered a standard molecular model of the FMO monomer described by the Hamiltonian  $H_{\text{mol}}$  and consisting of seven bacteriochlorophylls in the single-excitation subspace. Double excitation played no role at the considered weak spectroscopic field strengths. Recently, an eighth pigment in the FMO complex was found (54). However, its spatial distance from the other seven pigments is very large, and it is very likely that this pigment is removed in the majority of the complexes during the isolation procedure (17, 54). The model parameters (i.e., the site energies  $\epsilon_m$  and the electronic couplings  $J_{n,m}$ ) were taken from ref. 55. The spectral density of the bath is given in *SI Appendix*. During the procedure of fitting the model to the measured absorption and CD spectra, we kept the electronic coupling elements unchanged and optimized the site energies. To fit the absorption and CD spectra simultaneously, we optimized the site energies and the inhomogeneous broadening, which accounts for the static disorder. In particular, we chose a Gaussian distribution with a FWHM of  $90 \text{ cm}^{-1}$ , except for site 3, for which we found that it was necessary to reduce the static disorder to  $54 \text{ cm}^{-1}$  of FWHM to fit the absorption peak of  $12,150 \text{ cm}^{-1}$  at 77 K (the low-temperature calculations in comparison with the experimental spectra are shown in *SI Appendix*). To obtain converged results, 500 calculated spectra were included in the average. The orientations of the transition dipole moments were taken from Protein Data Bank ID code 3ENI (56), and the magnitudes of the transition dipole moments were assumed to all be 4 Debye. The modeling has been additionally verified (*SI Appendix*) by comparing the calculated results for the time-dependent FMO site populations with available exact numerical calculations (29).

**ACKNOWLEDGMENTS.** H.-G.D. thanks Eike-Christian Schulz for his comments on the properties of the FMO protein at room temperature. This work was supported by the Max Planck Society and the Hamburg Center for Ultrafast Imaging within the German Excellence Initiative supported by the Deutsche Forschungsgemeinschaft. H.-G.D. was supported generously by the Joachim-Hertz-Stiftung Hamburg. Work at the University of Glasgow was supported as part of the Photosynthetic Antenna Research Center, an Energy Frontier Research Center funded by the US Department of Energy, Office of Science, Basic Energy Sciences Award DE-SC0001035.

- Förster T (1948) Zwischenmolekulare energiewanderung und fluoreszenz. *Ann Phys* 437:55–75.
- Jang S, Newton M, Silbey RJ (2004) Multichromophoric Forster resonance energy transfer. *Phys Rev Lett* 92:218301.
- Engel GS, et al. (2007) Evidence for wavelike energy transfer through quantum coherence in photosynthetic systems. *Nature* 446:782–786.
- Panitchayangkoon G, et al. (2010) Long-lived quantum coherence in photosynthetic complexes at physiological temperature. *Proc Natl Acad Sci USA* 107:12766–12770.
- Collini E, et al. (2010) Coherently wired light-harvesting in photosynthetic marine algae at ambient temperature. *Nature* 463:644–647.
- Mukamel S (2000) Multidimensional femtosecond correlation spectroscopies of electronic and vibrational excitations. *Annu Rev Phys Chem* 51:691–729.
- Woutersen S, Hamm P (2002) Nonlinear two-dimensional vibrational spectroscopy of peptides. *J Phys Condens Mat* 14:R1035.
- Jonas DM (2003) Two-dimensional femtosecond spectroscopy. *Annu Rev Phys Chem* 54:425–463.
- Fenna RE, Matthews BW, Olson JM, Shaw EK (1974) Structure of a bacteriochlorophyll-protein from the green photosynthetic bacterium *Chlorobium limicola*: Crystallographic evidence for a trimer. *J Mol Biol* 84:231–240.
- Ball P (2011) Physics of life: The dawn of quantum biology. *Nature* 474:272–274.
- Scholes GD, Fleming GR, Olaya-Castro A, van Grondelle R (2011) Lessons from nature about solar light harvesting. *Nat Chem* 3:763–774.
- Lambert N, et al. (2013) Quantum biology. *Nat Phys* 9:10–18.
- Huelga SF, Plenio M (2013) Vibrations, quanta and biology. *Contemp Phys* 54:181–207.
- Mohseni M, Omar Y, Engel GS, Plenio M (2014) *Quantum Effects in Biology* (Cambridge Univ Press, Cambridge, MA).
- Abbott D, Davies P, Pati A (2010) *Quantum Aspects of Life* (World Scientific, Singapore).
- Olaya-Castro A, Nazir A, Fleming GR (2012) Quantum-coherent energy transfer: Implications for biology and new energy technologies. *Philos Trans R Soc Lond A Math Phys Eng Sci* 370:3613–3617.
- Thyrhaug E, Židek K, Dostál J, Bina D, Zigmantas D (2016) Exciton structure and energy transfer in the Fenna-Matthews-Olson complex. *J Phys Chem Lett* 7:1653–1660.
- Plenio M, Huelga SF (2008) Dephasing-assisted transport: Quantum networks and biomolecules. *New J Phys* 10:113019.
- Mohseni M, Rebentrost P, Lloyd S, Aspuru-Guzik A (2008) Environment-assisted quantum walks in photosynthetic energy transfer. *J Chem Phys* 129:174106.
- Olaya-Castro A, Lee CF, Fassioi Olsen F, Johnson NF (2008) Efficiency of energy transfer in a light-harvesting system under quantum coherence. *Phys Rev B* 78:085115.
- Thorwart M, Eckel J, Reina JH, Nalbach P, Weiss S (2009) Enhanced quantum entanglement in the non-Markovian dynamics of biomolecular excitons. *Chem Phys Lett* 478:234–237.
- Sarovar M, Ishizaki A, Fleming GR, Whaley KB (2010) Quantum entanglement in photosynthetic light-harvesting complexes. *Nat Phys* 6:462–467.
- Walschaers M, Fernandez-de-Cossio Diaz J, Mulet R, Buchleitner A (2013) Optimally designed quantum transport across disordered networks. *Phys Rev Lett* 111:180601.
- Wilde MM, McCracken JM, Mizel A (2010) Could light harvesting complexes exhibit non-classical effects at room temperature? *Proc Math Phys Eng Sci* 466:1347–1363.
- Briggs JS, Eisl A (2011) Equivalence of quantum and classical coherence in electronic energy transfer. *Phys Rev E* 83:051911.
- Miller WH (2012) Perspective: Quantum or classical coherence? *J Chem Phys* 136:210901.
- Mukamel S (2013) Comment on “Coherence and uncertainty in nanostructured organic photovoltaics”. *J Phys Chem A* 117:10563–10564.
- Halpin A, Johnson PJM, Miller RJD (2014) Comment on “Engineering coherence among excited states in synthetic heterodimer systems”. *Science* 344:1099.
- Nalbach P, Braun D, Thorwart M (2011) Exciton transfer dynamics and quantumness of energy transfer in the Fenna-Matthews-Olson complex. *Phys Rev E* 84:041926.
- Olbrich C, Strümpfer J, Schulten K, Kleinekathöfer U (2011) Theory and simulation of the environmental effects on FMO electronic transitions. *J Phys Chem Lett* 2:1771–1776.
- Christensson N, Kauffmann HF, Pullerits T, Mančal T (2012) Origin of long-lived coherences in light-harvesting complexes. *J Phys Chem B* 116:7449–7454.
- Kreisbeck C, Kramer T (2012) Long-lived electronic coherence in dissipative exciton dynamics of light-harvesting complexes. *J Phys Chem Lett* 3:2828–2833.
- Hossein-Nejad H, Olaya-Castro A, Scholes GD (2012) Phonon-mediated path-interference in electronic energy transfer. *J Chem Phys* 136:024112.
- Kolli A, O'Reilly EJ, Scholes GD, Olaya-Castro A (2012) The fundamental role of quantized vibrations in coherent light harvesting by cryptophyte algae. *J Chem Phys* 137:174109.
- Nalbach P, Thorwart M (2012) The role of discrete molecular modes in the coherent exciton dynamics in FMO. *J Phys B At Mol Opt Phys* 45:154009.
- Chin AW, et al. (2013) The role of non-equilibrium vibrational structures in electronic coherence and recoherence in pigment-protein complexes. *Nat Phys* 9:113–118.
- O'Reilly EJ, Olaya-Castro A (2014) Non-classicality of molecular vibrations activating electronic dynamics at room temperature. *Nat Comm* 5:3012.
- Mujica-Martinez C, Nalbach P (2015) On the influence of underdamped vibrations on coherence and energy transfer times in light-harvesting complexes. *Ann Phys* 527:592–600.
- Butkus V, Valkunas L, Abramavicius D (2014) Vibronic phenomena and exciton-vibronical interference in two-dimensional spectra of molecular aggregates. *J Chem Phys* 140:034306.
- Halpin A, et al. (2014) Two-dimensional spectroscopy of a molecular dimer unveils the effects of vibronic coupling on exciton coherences. *Nat Chem* 6:196–201.

41. Duan HG, Nalbach P, Prokhorenko VI, Mukamel S, Thorwart M (2015) On the nature of oscillations in two-dimensional spectra of excitonically-coupled molecular systems. *New J Phys* 17:072002.
42. Wen J, Zhang H, Gross ML, Blankenship RE (2009) Membrane orientation of the FMO antenna protein from *Chlorobaculum tepidum* as determined by mass spectrometry-based footprinting. *Proc Natl Acad Sci USA* 106:6134–6139.
43. Prokhorenko VI (2012) Global analysis of multi-dimensional experimental data. *Eur Photochem Assoc News*:21–23.
44. Duan HG, et al. (2015) Two-dimensional electronic spectroscopy of light harvesting complex II at ambient temperature: A joint experimental and theoretical study. *J Phys Chem B* 119:12017–12027.
45. Butkus V, Zigmantas D, Valkunas L, Abramavicius D (2012) Vibrational vs. electronic coherence in 2D spectrum of molecular systems. *Chem Phys Lett* 545:40–43.
46. Egorova D (2008) Detection of electronic and vibrational coherences in molecular systems by 2D electronic photon echo spectroscopy. *Chem Phys* 347:166–176.
47. Mukamel S (1995) Continuous distribution of oscillators: Dephasing and relaxation. *Principles of Nonlinear Optical Spectroscopy* (Oxford Univ Press, Oxford), pp 221–226.
48. Hamm P, Zanni M (2011) Homogeneous and inhomogeneous dynamics. *Concepts Methods 2D Infrared Spectroscopy* (Cambridge Univ Press, Cambridge, UK), pp 152–164.
49. Lazonder K, Pshenichnikov MS, Wiersma DA (2007) Two-dimensional optical correlation spectroscopy applied to liquid/glass dynamics. *Ultrafast Phenomena XV, Proceedings of the 15th International Conference*, eds Corkum P, Jonas DM, Miller RJD, Weiner AM (Springer, Berlin), pp 356–358.
50. Mujica-Martinez C, Nalbach P, Thorwart M (2013) Quantification of non-Markovian effects in the Fenna-Matthews-Olson complex. *Phys Rev E* 88:062719.
51. Rätsep M, Freiberg A (2007) Electron-phonon and vibronic coupling in the FMO bacteriochlorophyll a antenna complex studied by difference fluorescence line narrowing. *J Lumin* 127:251–259.
52. Rätsep M, Cai Z-L, Reimers JR, Freiberg A (2011) Demonstration and interpretation of significant asymmetry in the low-resolution and high-resolution Qy fluorescence and absorption spectra of bacteriochlorophyll a. *J Chem Phys* 134:024506.
53. Prokhorenko VI, Picchiotti A, Maneshi S, Miller RJD (2015) Broadband electronic two-dimensional spectroscopy in the deep UV. *Ultrafast Phenomena XIX. Springer Proceedings in Physics*, eds Yamanouchi K, Cundiff S, de Vivie-Riedle R, Kuwata-Gonokami M, DiMauro L (Springer, Cham, Switzerland), Vol 16, pp 432–435.
54. Schmidt am Busch M, Müh F, El-Amine Madjet M, Renger T (2011) The eighth bacteriochlorophyll completes the excitation energy funnel in the FMO protein. *J Phys Chem Lett* 2:93–98.
55. Adolphs J, Renger T (2006) How proteins trigger excitation energy transfer in the FMO complex of green sulfur bacteria. *Biophys J* 91:2778–2797.
56. Tronrud DE, Wen J, Gay L, Blankenship RE (2009) The structural basis for the difference in absorbance spectra for the FMO antenna protein from various green sulfur bacteria. *Photosynth Res* 100:79–87.